JOURNAL OF NATURAL PRODUCTS

Article

pubs.acs.org/jnp

Chiroptical Spectroscopy of Natural Products: Avoiding the Aggregation Effects of Chiral Carboxylic Acids

Prasad L. Polavarapu,*[,†] Emily A. Donahue,[†] Karissa C. Hammer,[†] Vijay Raghavan,[†] Ganesh Shanmugam,[†] Ibrahim Ibnusaud,[‡] Divya S. Nair,[‡] Chithra Gopinath,[‡] and Deenamma Habel[‡]

[†]Department of Chemistry, Vanderbilt University, Nashville, Tennessee 37235, United States

[‡]Institute for Intensive Research In Basic Sciences, Mahatma Gandhi University, P.D. Hills PO, Kottayam, Kerala, India 686 560

ABSTRACT: Determination of the absolute configurations and predominant conformations of chiral natural products, occurring as carboxylic acids, using chiroptical spectroscopic methods becomes challenging due to the formation of solute aggregates (in the form of dimers, etc.) and/or solute−solvent complexes resulting from intermolecular hydrogen bonding with solvent. A hypothesis that such aggregation effects can be avoided by using corresponding sodium salts or acid anhydrides for chiroptical spectroscopic measurements has been tested. For this purpose, vibrational circular dichroism, electronic circular dichroism, and optical rotatory dispersion spectra for disodium salts of two natural products, hibiscus acid and garcinia acid, and the anhydride of acetylated garcinia acid have been measured. These experimental spectra are analyzed in combination with quantum chemical calculations of corresponding spectra. The spectral analysis for sodium salts and anhydride turned out to be simpler, suggesting that the conversion of carboxylic acids to corresponding salts or anhydride can be advantageous for the application of chiroptical spectroscopy.

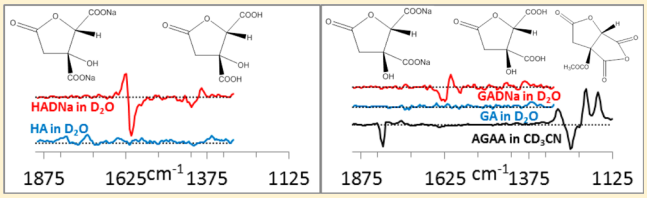

A large number of natural products occur as chiral carboxylic acids. While lactic acid (found in sour milk), tartaric acid (found in avocados), and malic acid (found in a variety of fruits such as apples) are well-known chiral carboxylic acids occurring in nature, new chiral carboxylic acids have recently been reported.[1,2] Hibiscus acid [(2*S*,3*R*)-3-hydroxy-5-oxo-tetrahydrofuran-2,3-dicarboxylic acid, **1**] and garcinia acid [(2*S*,3*S*)-3-hydroxy-5-oxo-tetrahydrofuran-2,3-dicarboxylic acid, **2**] (see Scheme 1) are two examples of natural products occurring as carboxylic acids.[1] Hibiscus acid (HA) is extracted from the calyxes/leaves of *Hibiscus sabdariffa* (Mathippuli-Roselle plant). Garcinia acid (GA) is extracted from the dried rind of the fruit of *Garcinia cambogia,* popularly known as "Malabar tamarind". Chiroptical spectroscopic methods are being widely used to determine the absolute configuration of natural products.[3−8] The interpretation of experimental chiroptical spectroscopic data is often undertaken with simultaneous quantum chemical predictions[9−13] of the corresponding chiroptical spectra. The solvent environment in which the experimental data are collected has to be mimicked or reproduced in quantum chemical calculations to achieve reliable predictions. When nonpolar and non-hydrogen-bonding solvents are used for spectroscopic measurements, the solvent environment for nonaggregating solutes can often be simulated with vacuum calculations. When polar and non-hydrogen-bonding solvents are used for spectroscopic measurements, the solvent environment for nonaggregating solutes can often be simulated using the polarizable continuum model (PCM).[14−17] However, when polar/nonpolar and non-hydrogen-bonding solvents are used for spectroscopic measurements on carboxylic acids, molecular aggregation (in the form of dimers or higher -mers) can often dominate, which requires the calculation of chiroptical spectra for dimers.[18,19] To avoid dimer formation, or due to the limitations of solubility of carboxylic acids in organic solvents, hydrogen-bonding solvents such as H_2O and DMSO become the common solvents used for their spectroscopic measurements. In these solvents, the carboxylic group often participates in hydrogen bonding with the solvent, which requires the consideration of solute−solvent clusters or solute−solvent molecular complexes for quantum chemical calculations.[20−22] The formation of dimers and their higher order analogues or hydrogen-bonded complexes with solvent is collectively referred to here as aggregation. Effects arising from aggregation lead to complexities in modeling the environment, which in turn requires demanding computational facilities, especially when dealing with large solute molecules, for achieving reliable quantum chemical predictions.

One of the alternatives used in the past to avoid these problems was to convert the carboxylic acids to corresponding methyl esters and conduct experimental investigations on these esters.[23−26] Since esters can be solubilized in non-hydrogen-bonding solvents such as CCl_4 and CH_2Cl_2, significant intermolecular interactions are avoided. This situation is favorable for quantum chemical calculations since the solvent environment with these solvents can often be represented by vacuum or PCM, and such calculations would often suffice for interpreting the experimental spectra.

Received: May 12, 2012
Published: August 9, 2012

dx.doi.org/10.1021/np300341z | *J. Nat. Prod.* 2012, 75, 1441−1450

Scheme 1

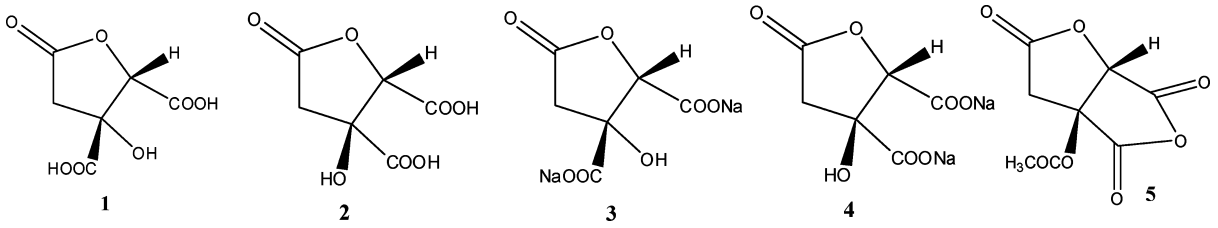

Table 1. Lowest Energy Conformations of HADNa at the B3LYP/aug-cc-pVDZ-PCM Level

conformer[a]	puckering angle, OC(=O)CC	Na_1–O (cis to O_{ring})	Na_1–O (trans to O_{ring})	Na_2–O (trans to O_{ring})	Na_2–O (cis to O of OH)	Na_1–O(H)	Gibbs energy	population
A	−17.2	2.38	2.42	2.28	2.33		−1082.5577	0.76
B	−16.8	2.31		2.28	2.34	2.45	−1082.5567	0.24

[a]Both conformers have an intramolecular hydrogen bond between O–H and C=O at the same stereogenic center; conformer A was found through both a manual search and using the Spartan program (followed by B3LYP/aug-cc-pVDZ-PCM optimizations).

In this article we explore alternate approaches to avoid aggregation effects resulting from hydrogen-bonding interactions in carboxylic acids in analyzing their chiroptical spectra. In these approaches, a chiral carboxylic acid is converted to its corresponding sodium salt or acid anhydride. In the case of sodium salts, due to the association of the Na^+ cation with the COO^- group, two advantages arise: (a) molecular aggregation is avoided (assuming that salts do not possess surfactant properties and form micelles[27]) and (b) the aqueous medium surrounding the salt may be represented, hopefully satisfactorily, by PCM, in which case it may be possible to avoid calculations on solute–solvent clusters. When carboxylic groups of dicarboxylic acids are converted into anhydrides, the resulting solutes are suitable for use with non-hydrogen-bonding solvents. In this article, we investigate the advantages and disadvantages of using sodium salts and acid anhydrides for determining the absolute configurations of chiral carboxylic acids using chiroptical spectroscopic methods. For this purpose, we consider disodium (2*S*,3*R*)-3-hydroxy-5-oxo-tetrahydrofuran-2,3-dicarboxylate (hibiscus acid disodium salt, HADNa, **3**) and disodium (2*S*,3*S*)-3-hydroxy-5-oxo-tetrahydrofuran-2,3-dicarboxylate (garcinia acid disodium salt, GADNa, **4**). In addition, (3a*S*,6a*S*)-2,4,6-trioxo-hexahydrofuro[3,4-*b*]furan-3a-yl acetate (acetylated garcinia acid anhydride, AGAA, **5**), the anhydride of acetylated **2**, is also investigated. The absolute configurations of **1** and **2** are known;[1,28,29] thus one can verify whether these configurations can be confirmed from the analysis of chiroptical spectroscopic data of **3**, **4**, and **5**. In compounds **3** and **4** there remains one OH group at C-3 that can participate in hydrogen bonding. However, this OH group does not influence the conclusions reached in this paper. In cases where the influence of such OH groups also needs to be avoided, the corresponding acetates[23,30] (as is the case for **5**) or methyl ether has to be considered.

RESULTS AND DISCUSSION

Conformational Analysis. Finding all possible low-energy conformations for sodium salts of small-ring molecules is a nontrivial task for two reasons. (a) Since there is no directional bonding between the Na^+ and COO^- ions, varying relative orientations of these oppositely charged ions are possible (vide infra). (b) It is necessary to undertake conformational analysis of ring systems carefully[25,26] because of the puckering of five-membered rings.

Hibiscus Acid Disodium Salt. We used two different procedures to identify the low-energy conformers of HADNa. (1) *Manual search*: We built eight plausible structures of hibiscus acid, four each with positive and negative puckering angles, replaced the H atom of the COOH group with Na, and began the geometry optimizations using the Gaussian 09 program[31] using the B3LYP functional[32] and 6-31G(d) basis sets.[33] All of these converged to two different conformations, with positive and negative puckering angles, respectively. The puckering angles of these optimized geometries were changed to opposite sign and reoptimized at the B3LYP/6-31G(d) level. However, the puckering values reverted back to those before sign reversal during optimization. Thus, only two conformations, with positive and negative puckering angles, respectively, were found, and these were further optimized at the B3LYP/aug-cc-pVDZ[34] and B3LYP/aug-cc-pVDZ/PCM(H_2O) levels, where PCM(H_2O) represents PCM for H_2O as the solvent. The conformer with a positive puckering angle turned out to have higher energy and negligible population. Next we performed a relaxed potential energy surface (PES) scan on this higher energy structure by varying the ring puckering angle in 5° increments. This PES scan led to another low-energy conformer with negative puckering angle. The two conformations with negative puckering angles turned out to be the low-energy conformers and are summarized in Table 1. To evaluate if all possible conformations have been identified, we used two different conformational search programs. (2) *Conformational search using the SPARTAN program*:[35] When default options are used,[36] this program searches for conformations by changing the torsional angles of rotatable bonds, but may not use the variation of five-membered ring puckering angles[37] as a viable option in the conformational search. As a consequence, the inversion of the ring puckering angle (that is, a change in the sign of the ring puckering angle) could not be realized. We incorporated additional options[37] for changing the puckering angles during the conformational search and used one geometry with positive puckering angle and another with negative puckering angle, separately, as the starting geometries to find low-energy conformers within a 20 kcal/mol energy range. In this procedure, the starting geometry with negative puckering angle led to seven conformations with negative puckering angles, and the starting geometry with positive puckering angle led to two conformations with positive puckering angles. These nine conformations were further

dx.doi.org/10.1021/np300341z | J. Nat. Prod. 2012, 75, 1441–1450

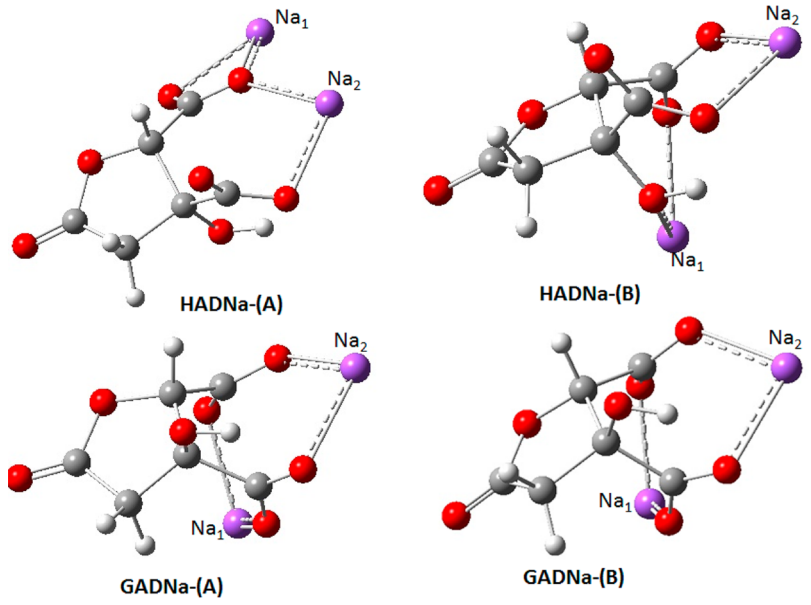

Figure 1. Lowest energy structures of HADNa (top) and GADNa (bottom) at the B3LYP/aug-cc-pVDZ/PCM(H_2O) level. Sodium ions are labeled as 1 and 2 to assist in identifying the distances listed in Tables 1 and 2. To enhance the perspective of the orientation of Na^+ ions, partial double bonds are drawn to these ions.

Table 2. Lowest Energy Conformations of GADNa at the B3LYP/aug-cc-pVDZ-PCM Level

conformer[a]	puckering angle, OC(=O)CC	Na_1–O (cis to O_{ring})	Na_1–O (trans to O_{ring})	Na_1–O (trans to O of OH)	Na_2–O (trans to O_{ring})	Na_2–O (cis to O of OH)	Na_2–O (trans to O of OH)	Gibbs energy	population
A	10.31	2.32		2.30	2.29	2.37		−1082.5565	0.52
B	−13.27	2.30		2.30	2.29	2.37		−1082.5562	0.39
C	15.68	2.39	2.41		2.34	2.52	2.50	−1082.5549	0.09

[a]All thee conformers have an intramolecular hydrogen bond between O–H and C=O at the same stereogenic center; conformers A and B were found through both manual search and using the Spartan program (followed by B3LYP/aug-cc-pVDZ-PCM optimizations).

optimized at the B3LYP/aug-cc-pVDZ/PCM(H_2O) level. Among these nine optimized geometries, the conformers with positive puckering angles had higher relative energies and negligible populations. One conformation with a negative puckering angle was populated to a 98% level. This conformation is also the lowest energy conformer found through manual search (Table 1). Note that a second low-energy conformer, found through a relaxed PES scan of a manual search, could not be obtained through the conformational search using the SPARTAN program and subsequent B3LYP optimizations. (3) *Conformational search using the CONFLEX program*:[38] This program by default[39] searches for conformations that differ in ring puckering angles. However, the conformational search yielded unrealistic geometries with Na^+ ions far removed from the rest of the molecule. Following communications with CONFLEX technical support we decided that the CONFLEX program is not suitable for conformational search of ionic species, and this deficiency in the CONFLEX program has been noted previously.[40]

The two lowest energy conformers of HADNa are shown in Figure 1. One would normally expect each sodium cation to be near a carboxylate group, perhaps symmetrically placed between the two oxygen atoms of the carboxylate anion. However, the structures shown in Figure 1 defy this common assumption. In conformer A, one sodium ion (Na_1) is located between two oxygen atoms of one carboxylate anion, but the second sodium ion (Na_2) is located between one oxygen atom of the carboxylate anion (that is already associated with Na_1) and an oxygen atom of another carboxylate group. This leaves one oxygen atom of a carboxylate group far away from sodium ions. In conformer B, Na_1 is located between the OH oxygen atom and an oxygen atom of a carboxylate group and Na_2 is located between oxygen atoms of different carboxylate groups. This leaves one oxygen atom of a carboxylate group far away from sodium ions.

Garcinia Acid Disodium Salt. (1) *Manual search*: We built eight plausible structures of garcinia acid, four each with positive and negative puckering angles, replaced the H atom of the COOH group with Na, and began the geometry optimizations using the Gaussian 09 program at the B3LYP/6-31G(d) level. All of the resulting geometries had positive puckering angles. When the positive puckering angles in the optimized geometries of the two lowest energy conformers were changed to negative and reoptimized, the signs of the puckering angles reverted back to positive signs. A relaxed PES scan at the B3LYP/6-31G(d) level yielded a low-energy conformer with a negative puckering angle and turned out to be lower in energy than the two conformers with positive puckering angles. These three conformations were further optimized at the B3LYP/aug-cc-pVDZ and B3LYP/aug-cc-pVDZ/PCM(H_2O) levels. The conformers optimized at the B3LYP/aug-cc-pVDZ/PCM(H_2O) level are summarized in Table 2. To evaluate if all possible conformations have been identified, we next used a conformational search program as described below (2) *Conformational search using the SPARTAN program*: In addition to the above-mentioned manual search

dx.doi.org/10.1021/np300341z | J. Nat. Prod. 2012, 75, 1441–1450

method we also used a conformational search using the SPARTAN program (with the same options as were used for HADNa). As for HADNa, two different starting geometries, one with positive puckering angle and the other with negative puckering angle, were used for the conformational search. One starting geometry led to nine conformations, while the other led to four (the latter four are also among the first nine conformers). However, unlike in HADNa, the conformational search yielded both positive and negative puckering angles for each of the starting geometries. These nine conformations were further optimized at the B3LYP/aug-cc-pVDZ/PCM(H_2O) level. This optimization yielded two low-energy conformers (one with positive puckering angle and the other with negative puckering angle), which are also the ones found through the manual search method.

The two lowest energy conformers, A and B, of GADNa are shown in Figure 1. Unlike in HADNa, these two lowest energy conformers have the sodium ions symmetrically located between oxygen atoms, but these oxygen atoms belong to two different carboxylate groups. The main difference between these two conformers is in the ring puckering angles (see Table 2).

There are significant differences in the populations of conformers at the B3LYP/aug-cc-pVDZ and B3LYP/aug-cc-pVDZ/PCM(H_2O) levels of calculations. While only one conformer (B of HADNa and GADNa) has significant population in the former calculation, two conformers (A and B of HADNa and GADNa) are found to have significant populations in the latter calculation (see Tables 1 and 2). Gas-phase geometry optimizations for disodium salts probably do not provide a realistic representation for solution-phase experimental studies in H_2O, and for this reason only geometries and chiroptical properties obtained using PCM-(H_2O) are reported in this work.

In summarizing the conformational analysis for sodium salts, it is necessary to emphasize that the commercial conformational search programs should not be taken as a sufficient means for identifying the low-energy conformations. Such search options should be supplemented with PES scans to ensure that all low-energy conformations have been identified.

Acetylated Garcinia Acid Anhydride. A conformational search with the CONFLEX program yielded three conformations, within 20 kcal/mol, differing in the orientation of the acetyl group (Figure 2a–c). These three conformations were further optimized at the B3LYP/6-31G(d) and B3LYP/aug-cc-pVDZ levels with and without using PCM for CH_3CN solvent influence (CH_3CN and CD_3CN are used for experimental measurements). In all cases, a single conformer was found to be the dominant one and the remaining two conformations had negligible populations. The PES scan at the B3LYP/6-31G(d) level by varying the puckering angles in each of the two rings of GAA indicated no other stable conformations.

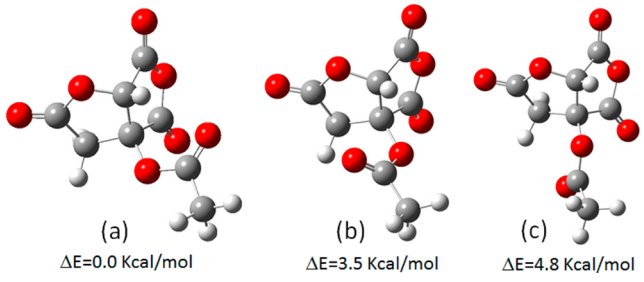

Figure 2. Three optimized conformers of AGAA at the B3LYP/aug-cc-pVDZ level.

Chiroptical Spectra of Disodium Salts. The experimental vibrational absorption (VA) and vibrational circular dichroism (VCD) spectra of HADNa (Figure 3) in D_2O are simple: one strong absorption band at 1616 cm^{-1} and an associated bisignate VCD couplet (positive and negative at 1624 and 1608 cm^{-1}, respectively). The population-weighted predicted absorption spectrum shows two bands, at 1641 and 1608 cm^{-1}, corresponding to one unresolved absorption band in the experimental spectrum at 1616 cm^{-1}, suggesting that the calculated bands have a larger separation than that seen in the experimental spectrum. The population-weighted predicted VCD spectrum does show a bisignate VCD couplet (positive at 1643 and negative at 1606 cm^{-1}) resembling the corresponding experimentally observed bisignate VCD couplet. As in the absorption spectrum, the positions of the two predicted VCD bands have a larger separation than that seen in the experimental spectrum.

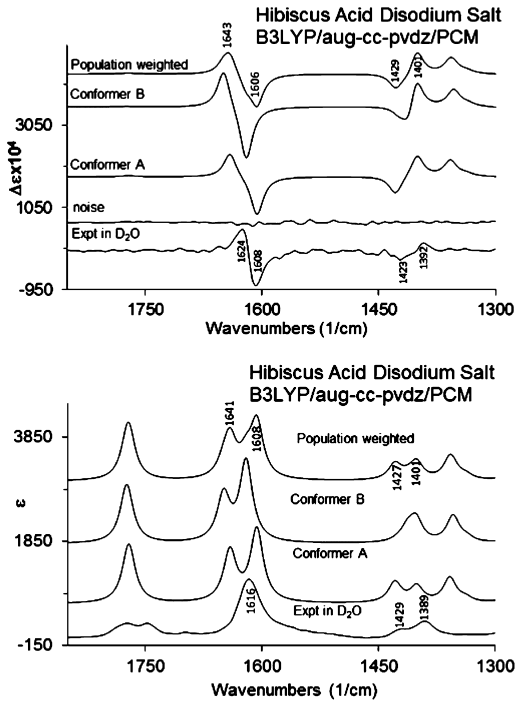

Figure 3. Comparison of experimental VCD (top) and VA (bottom) spectra of HADNa (17 mg/mL in D_2O; path length: 50 μm) with corresponding calculated spectra for the two lowest energy conformers and population-weighted spectra at the B3LYP/aug-cc-pVDZ/PCM-(H_2O) level. ε and $\Delta\varepsilon$ values are in units of L mol^{-1} cm^{-1}.

In addition to the above-mentioned stronger bands, a very weak negative VCD at 1423 cm^{-1} and positive VCD at 1392 cm^{-1}, associated with corresponding absorption bands at 1429 and 1389 cm^{-1}, respectively, are seen in the experimental spectra. The population-weighted predicted spectra show the corresponding VCD features at 1429 and 1401 cm^{-1}, with corresponding predicted absorption bands at 1427 and 1401 cm^{-1}.

On the basis of the observation that the predicted VCD spectrum for HADNa matches the experimental spectrum, the known absolute configuration of HA is supported by the VCD studies on its disodium salt.

dx.doi.org/10.1021/np300341z | J. Nat. Prod. 2012, 75, 1441–1450

The experimental VA and VCD spectra of GADNa (Figure 4) in D_2O are also simple: one strong absorption band at 1624

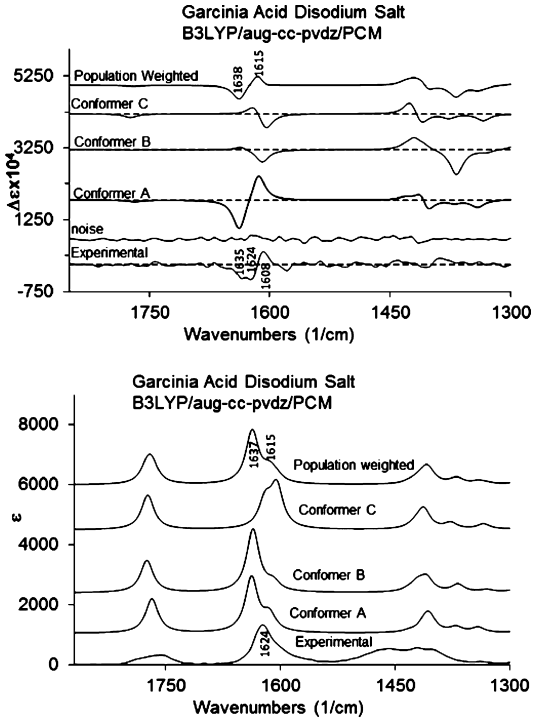

Figure 4. Comparison of experimental VCD (top) and VA (bottom) spectra of GADNa (12 mg/mL in D_2O; path length: 50 μm) with corresponding calculated spectra for the three lowest energy conformers and population-weighted spectra at the B3LYP/aug-cc-pVDZ/PCM(H_2O) level. ε and $\Delta\varepsilon$ values are in units of L mol^{-1} cm^{-1}.

cm^{-1} and an associated bisignate VCD couplet (negative VCD at higher frequency and positive VCD at lower frequency). This bisignate VCD couplet has an opposite sign pattern and weaker intensity than that seen for HADNa. The population-weighted predicted absorption spectrum shows two bands at 1637 and 1615 cm^{-1}, corresponding to one unresolved absorption band in the experimental spectrum at 1624 cm^{-1}. The calculated absorption bands, as in HADNa, have larger separation than the corresponding experimental bands. The population-weighted predicted VCD spectrum shows a bisignate VCD couplet (negative at 1638 and positive at 1615 cm^{-1}) resembling the corresponding experimentally observed VCD couplet. As can be seen from the predicted VCD spectra for individual conformers, conformer A has a VCD sign pattern that matches the experimental VCD sign pattern, while conformers B and C do not. Thus conformer A appears to be the most important one for GADNa .

On the basis of the observation that the predicted VCD spectrum for GADNa matches the experimental spectrum, the known absolute configuration of GA is supported by the VCD studies on its disodium salt. However, it should be noted that the VCD couplets observed for the two diastereomers (HADNa and GADNa) are of opposite signs (Figure 3 and 4). Thus it is not possible to differentiate between diastereomers and enantiomers of these compounds on the basis of VCD studies alone, as pointed out recently also for the esters of HA and GA.[26]

The experimental electronic absorption (EA) and electronic circular dichroism (ECD) spectra of HADNa are shown in Figure 5. The EA spectrum does not show a definite band

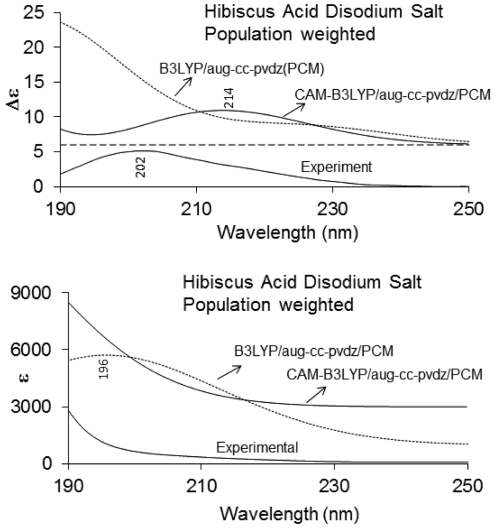

Figure 5. Comparison of experimental ECD (top) and EA (bottom) spectra of HADNa (3 mg/mL in H_2O) with corresponding calculated population-weighted spectra at the B3LYP/aug-cc-pVDZ/PCM(H_2O) and CAM-B3LYP/aug-cc-pVDZ/PCM(H_2O) levels. ε and $\Delta\varepsilon$ values are in units of L mol^{-1} cm^{-1}.

feature, but the ECD spectrum shows a well-defined Cotton effect with a positive sign at 202 nm. This positive ECD feature is reproduced in the predicted ECD spectrum with a red shift (CAM-B3LYP[41]/aug-cc-pVDZ/PCM(H_2O) level) or a blue shift (B3LYP/aug-cc-pVDZ/PCM(H_2O) level). The predicted absorption spectrum at the B3LYP/aug-cc-pVDZ/PCM(H_2O) level shows a well-defined absorption band at 196 nm, but not at the CAM-B3LYP/aug-cc-pVDZ/PCM(H_2O) level. The predictions at the CAM-B3LYP/aug-cc-pVDZ/PCM(H_2O) level are in line with the experimental observations. On the basis of this observation, the known absolute configuration of HA is supported by the ECD spectra of HADNa at the CAM-B3LYP/aug-cc-pVDZ/PCM(H_2O) level.

The experimental EA and ECD spectra of GADNa are shown in Figure 6. The experimental ECD spectrum also shows a positive Cotton effect at 200 nm, but there is no well-defined band in the EA spectrum. The predicted ECD spectrum at the CAM-B3LYP/aug-cc-pVDZ/PCM(H_2O) level shows a weak Cotton effect at 196 nm that is opposite in sign to the experimental Cotton effect. When the functional is changed to BHLYP,[42] the predicted ECD spectrum shows a Cotton effect with correct sign, but the magnitude is weak (note that the displayed spectrum is amplified ×3). Thus, the predicted ECD spectra are not as convincing as those for HADNa for supporting the absolute configuration through studies on GADNa. However, this is due to the small ECD magnitude predicted, and similar issues[25] were also noted in the analysis of ECD spectra of garcinia acid dimethyl ester. Note also that ECD Cotton effects are positive for both HADNa and GADNa, so the discrimination between diastereomers through ECD is less convincing.

The experimental specific rotation for HADNa is positive at all five wavelengths measured, with magnitudes increasing toward shorter wavelengths (Figure 7). The same trend is seen for the predicted specific rotations, at both the CAM-B3LYP/

dx.doi.org/10.1021/np300341z | J. Nat. Prod. 2012, 75, 1441−1450

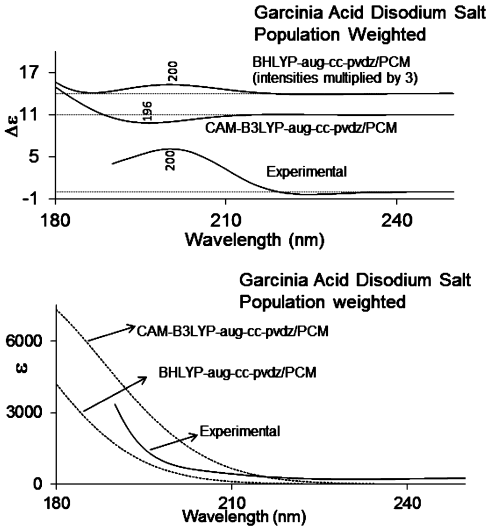

Figure 6. Comparison of experimental ECD (top) and EA (bottom) spectra of GADNa (3 mg/mL in H_2O) with corresponding calculated population-weighted spectra at the BHLYP/aug-cc-pVDZ/PCM-(H_2O) and CAM-B3LYP/aug-cc-pVDZ/PCM(H_2O) levels. ε and $\Delta\varepsilon$ values are in units of L mol^{-1} cm^{-1}.

aug-cc-pVDZ/PCM(H_2O) and B3LYP/aug-cc-pVDZ/PCM-(H_2O) levels, even though the magnitudes at the CAM-B3LYP/aug-cc-pVDZ/PCM(H_2O) level are closer to the experimental magnitudes. Thus, the known absolute configuration of hibiscus acid is supported by the optical rotatory dispersion (ORD) measurements on HADNa.

The experimental magnitudes of the specific rotation for GADNa are larger than those for HADNa, but the signs are the same for both GADNa and HADNa (see Figure 7). The predicted trend in specific rotation, at all three levels, namely, B3LYP/aug-cc-pVDZ/PCM(H_2O), CAM-B3LYP/aug-cc-pVDZ/PCM(H_2O), and BHLYP[42]/aug-cc-pVDZ/PCM(H_2O), are similar and match the trend observed in the experimental ORD data. Thus, the known absolute configuration of GA is supported by the ORD spectra of GADNa. However, the ORD is positive for both HADNa and GADNa, so the discrimination between diastereomers through ORD is less convincing.

Advantages and Disadvantages of Using Salts. To assess the advantages and disadvantages in using sodium salts, both experimental and computational aspects have to be considered. From an experimental viewpoint, it is necessary to assess if the magnitudes of experimental chiroptical signals are affected on going from carboxylic acid to its sodium salt. For this purpose, the experimental ECD and ORD spectra are compared in Figure 8 for the two acids and their salts. It is evident that the experimental ORD magnitudes of HADNa and GADNa are slightly smaller than those of corresponding acids. The experimental ECD magnitudes of HADNa and GADNa, however, are slightly greater than those of the corresponding acids. These small differences do not influence the selection of acid or its salt for experimental ECD and ORD measurements. However, for VA/VCD measurements in H_2O, due to strong interfering solvent infrared absorption at 1650 cm^{-1}, high concentrations and shorter path lengths (~6 μm) are needed. The use of D_2O as solvent permits path lengths up to ~50 μm (limited by strong absorption from D_2O at ~1250 cm^{-1}) and allows VA/VCD measurements in the 1900−1300 cm^{-1} region. Furthermore, since vibrational functional groups (carboxylic acid vs carboxylate anion) are different in acids and their salts, the experimental details will also differ. Carboxylic acids give IR absorption bands originating from the C=O group, while carboxylate anions give corresponding absorption bands originating from the COO^- group. These differences are reflected in the VA/VCD spectra for acids and their salts, as shown in Figure 9. The two salts HADNa and GADNa give bisignate couplets associated with COO^- stretching vibrations, but the corresponding acids HA and GA do not give any measurable VCD signals associated with the C=O stretching vibrational bands (even at a high concentration of 48 mg/mL). The lack of measurable VCD for HA and GA in D_2O may have to do with conformational averaging; that is, VCD associated with many possible conformations of solute−solvent complexes may average to a negligible sum. Even if measurable VCD signals were found for acids in D_2O, the computational analysis for acid−water clusters would have been complex. This comparison favors the VCD measurements for salts, at least in the present case, over parent acids. However, better VCD signals are obtained for HA and GA when DMSO-d_6 solvent is used, where lower solvent absorption interference allows VCD measurements down to 1150 cm^{-1} and the use of larger path lengths. The spectra measured in DMSO-d_6 at 10 mg/mL in the 1900−1700 cm^{-1} region and at 37 mg/mL for the 1700−1125 cm^{-1} region using a 100 μm path length are also shown in Figure 9. Although a wider spectral region and better signal-to-noise ratio could be realized for HA and GA in DMSO-d_6, carboxylic acids can form hydrogen bonds with DMSO-d_6, resulting in solute−solvent complexes. Modeling these complexes and investigating different structural variations of these complexes become unwieldy, and this disadvantage discourages VCD studies on carboxylic acids in DMSO-d_6. These observations suggest that although VCD measurements

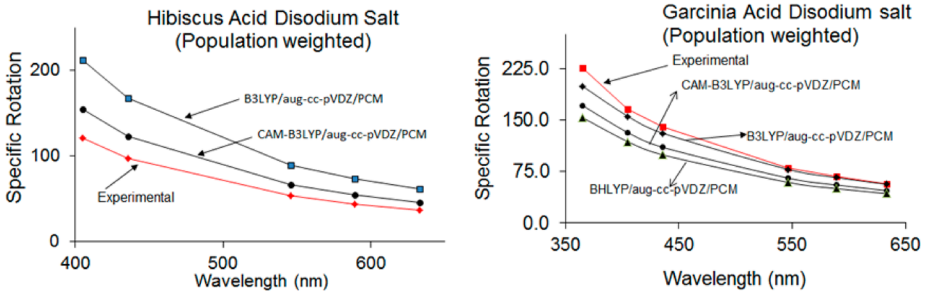

Figure 7. Comparison of experimental ORD spectra of HADNa (left) and GADNa (right) (both at 3 mg/mL in H_2O) with corresponding calculated population-weighted spectra at the B3LYP/aug-cc-pVDZ/PCM(H_2O) and CAM-B3LYP/aug-cc-pVDZ/PCM(H_2O) levels. An additional calculation at the BHLYP/aug-cc-pVDZ/PCM(H_2O) level is also used for GADNa. Specific rotations are in units of deg cm^3 g^{-1} dm^{-1}.

dx.doi.org/10.1021/np300341z | J. Nat. Prod. 2012, 75, 1441−1450

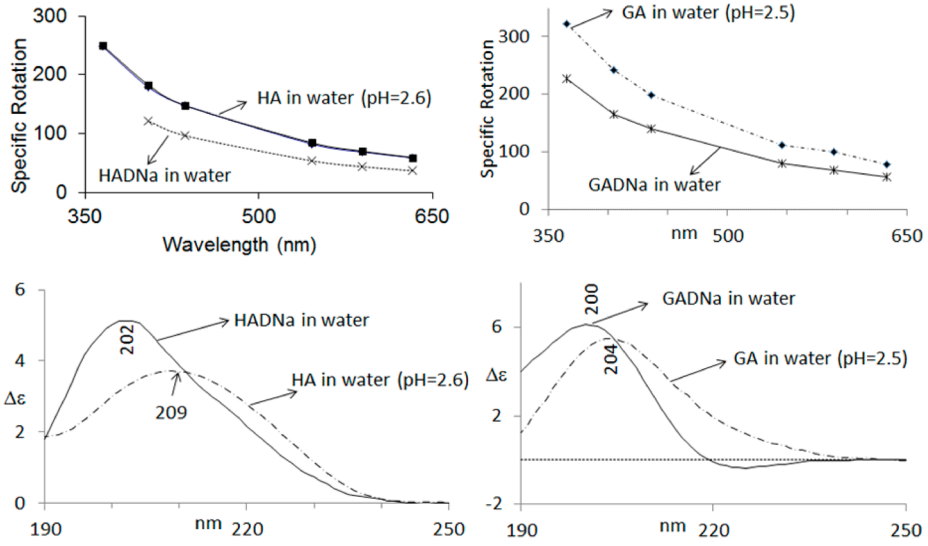

Figure 8. Comparison of the ECD (bottom) and ORD (top) spectra of hibiscus acid (HA), garcinia acid (GA), and their sodium salts, HADNa and GADNa. All spectra were measured at ~3 mg/mL in H_2O. ε and $\Delta\varepsilon$ values are in units of L mol^{-1} cm^{-1}. Specific rotations are in units of deg cm^3 g^{-1} dm^{-1}.

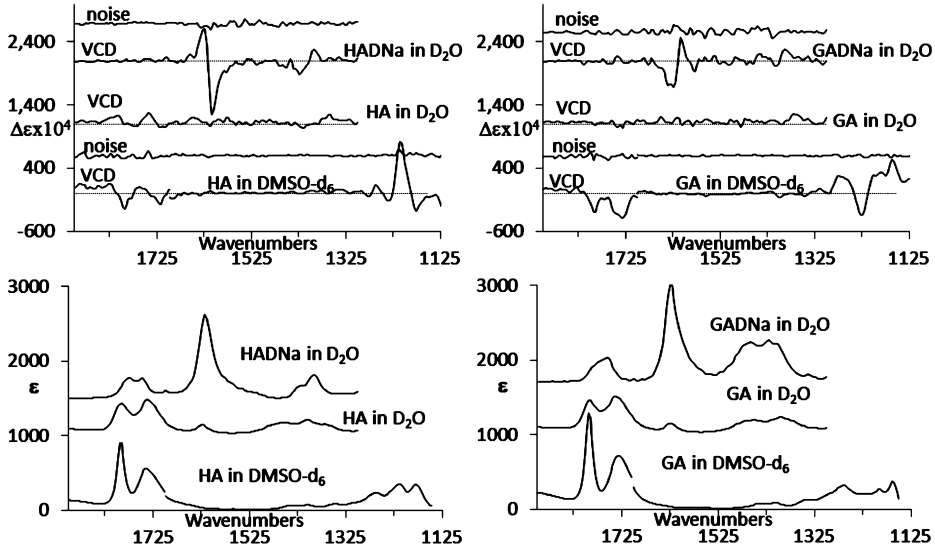

Figure 9. Comparison of VA (top) and VCD (bottom) spectra of HADNa, GADNA, and corresponding acids. The spectra of HA in D_2O were measured at 48 mg/mL using a 50 μm path length cell, and those in DMSO-$d_6$were measured at 10 mg/mL (for the 1900−1700 cm^{-1}) region and at 35 mg/mL (1700−1150 cm^{-1}), both using 100 μm path length cells. The spectra of GA in D_2O were measured at 48 mg/mL using a 50 μm path length cell, and those in DMSO-d_6 were measured at 10 mg/mL (1900−1700 cm^{-1}) and at 37 mg/mL (1700−1150 cm^{-1}), both using 100 μm path length cells. ε and $\Delta\varepsilon$ values are in units of L mol^{-1} cm^{-1}.

on HADNa and GADNa in D_2O can result in a limited accessible spectral region, the disadvantages arising from demanding computational analysis do not favor VCD analysis for HA and GA in D_2O or DMSO-d_6 solvents. Therefore, definite advantages are evident for undertaking chiroptical spectroscopic studies for HADNa and GADNa instead of their parent acids, HA and GA. However, these observations should not be generalized for all carboxylic acids because there may be cases where sodium salts may not give measurable VCD signals but their parent acids might. Therefore, it is important to verify the advantages/disadvantages of using sodium salts for individual cases.

Chiroptical Spectra of Acetylated Garcinia Acid Anhydride. The experimental VA and VCD spectra of AGAA are compared to the corresponding predicted spectra at the B3LYP/aug-cc-pVDZ and B3LYP/aug-cc-pVDZ/PCM-(CH_3CN) levels in Figure 10. The experimental spectra obtained in CD_3CN and CD_2Cl_2 are similar. Since there is only one predominant conformer for AGAA, all calculations were done for this one predominant conformer (see Figure 2a). The calculations with PCM(CH_3CN) reproduce the experimental spectra better than those without PCM. The experimental VCD spectra show bands at 1809(−), 1288(+), 1250(−), 1203(+), and 1169(+) cm^{-1}, and these features are well reproduced in the calculated spectrum at the B3LYP/aug-cc-pVDZ/PCM(CH_3CN) level respectively at 1825(−), 1293(+), 1245(−), 1208(+), and 1167(+) cm^{-1}. ECD and EA spectra calculated for AGAA at the CAM-B3LYP/aug-cc-pVDZ, CAM-B3LYP/aug-cc-pVDZ/PCM(CH_3CN), BHLYP/aug-cc-pVDZ, and BHLYP/aug-cc-pVDZ/PCM(CH_3CN) lev-

dx.doi.org/10.1021/np300341z | J. Nat. Prod. 2012, 75, 1441−1450

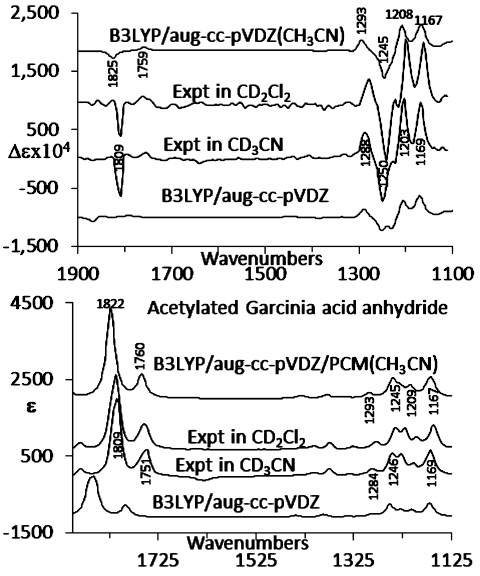

Figure 10. Comparison of experimental VCD (top) and VA (bottom) spectra of AGAA (15 mg/mL in CD_3CN; 8 mg/mL in CD_2Cl_2) with corresponding calculated spectra for the lowest energy conformer at the B3LYP/aug-cc-pVDZ and B3LYP/aug-cc-pVDZ/PCM(CH_3CN) levels. ε and $\Delta\varepsilon$ values are in units of L mol^{-1} cm^{-1}.

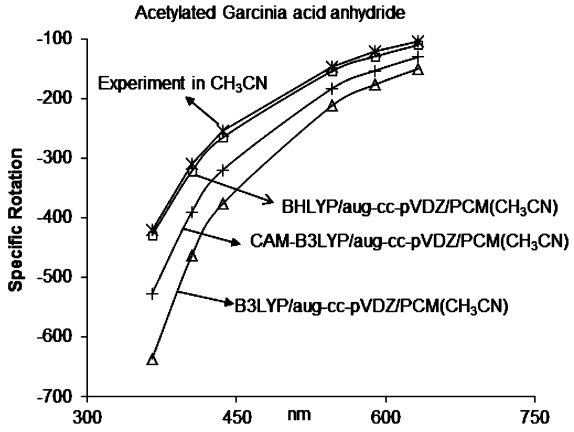

Figure 12. Comparison of experimental ORD spectra of AGAA with corresponding calculated spectra for the lowest energy conformer at different levels of theory. The spectra were calculated with the aug-cc-pVDZ basis set. The experimental spectra were measured at ~3 mg/mL in CH_3CN. Specific rotations are in units of deg cm^3 g^{-1} dm^{-1}.

els are shown in Figure 11. The experimental ECD spectrum shows one broad negative Cotton effect covering the 190−260 nm region, and the calculated spectra also show a broad negative Cotton effect. The ORD spectra calculated with the aug-cc-pVDZ basis set, PCM(CH_3CN), and three different density functionals (B3LYP, CAM-B3LYP, BHLYP) are compared to the experimental ORD spectra in Figure 12. Those calculated at the BHLYP/aug-cc-pVDZ/PCM(CH_3CN) level are in a near perfect match with the experimental values, although those at the B3LYP/aug-cc-pVDZ/PCM(CH_3CN) and CAM-B3LYP/aug-cc-pVDZ/PCM(CH_3CN) levels are also close to the experimental values.

In conclusion, three different chiroptical protocols (VCD, ECD, and ORD) confirm that the absolute configuration of GA may be deduced from analysis of the spectra of its anhydride.

Advantages and Disadvantages of Using Acid Anhydrides. There are three advantages to using anhydrides for chiroptical spectroscopic analysis. (a) the conformational flexibility and intramolecular hydrogen bonding effects have been completely eliminated. As a result, only one predominant conformation is present for AGAA and this led to significantly reduced spectral complexity (b) a non-hydrogen bonding solvent (CD_2Cl_2) may be used for experimental measurements whose solvent environment can be represented by PCM. Even though CD_3CN may participate in hydrogen bonding (with N as the electron donor), the spectra of AGAA in CD_3CN are similar those in CH_2Cl_2, because there are no acceptor OH groups in AGAA to form hydrogen bonds with CD_3CN (c) restricted conformational mobility also leads to larger chiroptical signals. The disadvantages of using anhydrides are

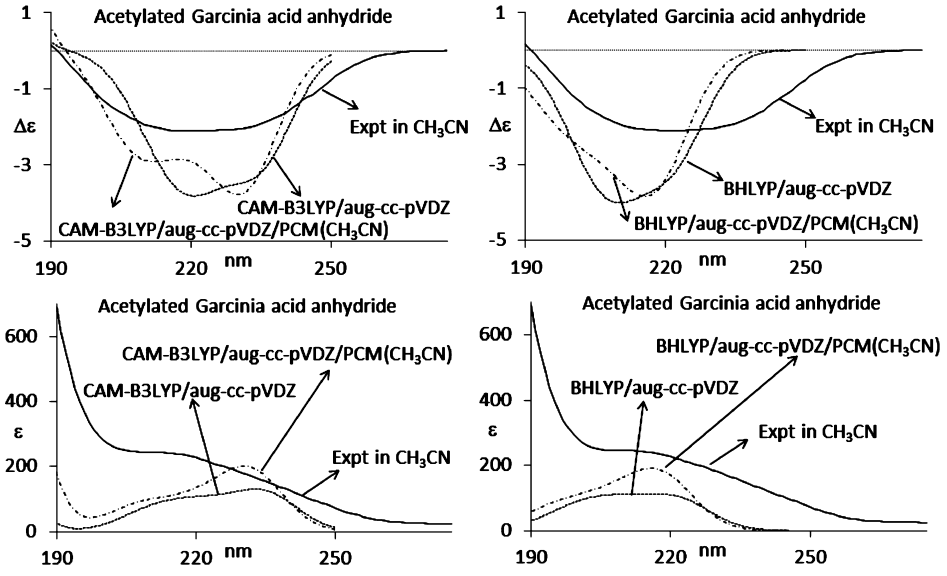

Figure 11. Comparison of experimental ECD (top) and EA (bottom) spectra of AGAA with corresponding calculated spectra for the lowest energy conformer at different levels of theory. The experimental spectra were measured at ~3 mg/mL in CH_3CN. ε and $\Delta\varepsilon$ values are in units of L mol^{-1} cm^{-1}.

dx.doi.org/10.1021/np300341z | J. Nat. Prod. 2012, 75, 1441−1450

as follows: (a) anhydrides can react with trace amounts of H_2O, so one needs to take precautions and avoid water contamination. Even then, atmospheric water can initiate the conversion of anhydride to its parent acid, but this reaction is usually slow. Within ~3−4 h after the preparation of solution in closed cells, reaction with atmospheric moisture does not influence the measurements, but over extended periods of time (~24 h) hydrolysis is occurring (b) in order to form an acid anhydride two carboxylic acid groups are needed and these two carboxylic acid groups should be present in a favorable disposition. This basic requirement rules out monocarboxylic acids, and some dicarboxylic acids as well, from conversion to anhydrides. Compound **1** is an example of dicarboxylic acid where the trans-disposition of two carboxylic acid groups does not allow the formation of its anhydride.

■ CONCLUSIONS

The use of sodium salts for determining the absolute configuration of its parent acid eliminates the complexities arising from hydrogen bonding interactions between solvent and acid. The use of the anhydride of a dicarboxylic acid is even more advantageous due to the elimination of conformational flexibility and hydrogen bonding interactions with solvent.

■ EXPERIMENTAL SECTION

General Experimental Procedures. General procedure for the preparation of **3** and **4** is as follows: To an aqueous solution of HA or GA (2.0 g, 10.5 mmol, in 10 mL H_2O), saturated aqueous $NaHCO_3$ was added until the pH of the reaction mixture was neutral. The residue obtained after evaporation of the reaction mixture under reduced pressure, was triturated and washed with dry acetone (5 × 20 mL). The product was finally dried under vacuum to give a colorless solid. The procedure for preparation of **5** is as follows: To 1 g (4.7 mmol) of garcinia acid in a round-bottom flask was added 4 mL of acetyl chloride and the mixture was refluxed for 1.5−2.0 h until all the acid dissolved. The solution was allowed to cool undisturbed and was finally chilled in ice bath. The acetylated garcinia acid anhydride separated out as white crystals and was decanted. The crystals were washed several times with dry n-hexane and dried in vacuum.

The optical rotations at six discrete wavelengths (633, 589, 546, 436, 405, 365 nm) were measured, for HADNa, GADNa, HA, GA, and AGAA, all at a concentration of ~3 mg/mL with a 0.5 dm cell using an Autopol IV polarimeter. CH_3CN was the solvent for AGAA and H_2O for all others. The optical rotation reading at 365 nm was not stable for HADNa. The EA and ECD spectra were recorded for HADNa, GADNa, HA, GA, and AGAA, all at a concentration of ~3 mg/mL in H_2O using a 0.01 cm path length quartz cell on a Jasco J720 spectrometer. Acetonitrile was the solvent for AGAA and H_2O for all others. The solvent spectrum has been subtracted from the experimental ECD spectra of sample solution.

The vibrational absorption and VCD spectra were recorded in the 2000−900 cm^{-1} region using a commercial Fourier Transform VCD spectrometer, which has been modified and recently aligned to accommodate double polarization modulation.[43] VA and VCD spectra were measured at concentrations of 17 mg/mL (HADNa), ~12 mg/mL (GADNa), 48 mg/mL(HA) and 48 mg/mL(GA) in D_2O using a 50 μm fixed path length cell with BaF_2 windows and 3 h data collection time (1 h for HA and GA). The region below 1300 cm^{-1} has been excluded from presentation for the spectra measured in D_2O due to interference from D_2O absorption. VA and VCD spectra were obtained in DMSO-d_6 for both HA and GA, at 10 mg/mL (as well as 37 mg/mL) concentrations using a 100 μm path length cell with BaF_2 windows and 1 h data collection time. The VA and VCD spectra for AGAA were obtained in CD_3CN (15 mg/mL) and CD_2Cl_2 (8 mg/mL) using a 100 μm path length cell with BaF_2 windows. In the VA spectra, the solvent absorption was subtracted. Similarly, the VCD spectrum measured for the solvent was subtracted from that of the sample solution. All VCD spectra were recorded at 8 cm^{-1} resolution.

Computational Details. *VCD Spectra.* VCD calculations were undertaken using the B3LYP[32] functional and the aug-cc-pVDZ basis set[34] using the polarizable continuum model (PCM),[17] as recently implemented in the Gaussian 09 program.[31] VCD calculations using PCM were performed at the respective optimized geometries and are designated as B3LYP/aug-cc-pVDZ/PCM. The theoretical VA and VCD spectra were simulated with Lorentzian band shapes of 10 cm^{-1} half-width at half-peak height. Populations of conformers derived from Gibbs free energies were used to obtain the population weighted VCD spectra. *ECD Spectra*: Two levels of calculations using B3LYP, and CAM-B3LYP[41] with aug-cc-pVDZ basis set and PCM were undertaken for ECD calculations. The geometries optimized in B3LYP calculation were used for CAM-B3LYP calculations. The calculations performed for ECD are designated as B3LYP/aug-cc-pVDZ/PCM, CAM-B3LYP/aug-cc-pVDZ/PCM to represent solution phase results. The predicted electronic transition energies obtained with the B3LYP functional are generally lower[44] than the corresponding experimental values. This deficiency is corrected with CAM-B3LYP functionals[41] which provide a better description of the tails of electronic density and hence of excited electronic states. For GADNa and AGAA an additional level of calculation using the BHLYP functional[42] was also undertaken and designated as BHLYP/aug-cc-pVDZ/PCM. The theoretical EA and ECD spectra were simulated from the first 25 singlet → singlet electronic transitions using Gaussian band shapes and 20 nm half-width at 1/e of peak height. Rotational strength values, calculated in the velocity representation, have been used for ECD spectral simulations. The EA spectral intensities have been derived from dimensionless oscillator strengths. Populations of conformers derived from the Gibbs free energies were used to obtain the population weighted ECD spectra. *ORD Spectra*: The functionals and basis set used for ORD calculation are the same as those used for ECD calculations. Optical rotations at six different wavelengths were calculated. The experimental optical rotation at 365 nm for HADNa was not stable, so this data point is not shown for HADNa.

■ AUTHOR INFORMATION

Corresponding Author

*E-mail: Prasad.L.Polavarapu@Vanderbilt.edu. Phone: (615) 322-2836. Fax: (615) 322-4936.

Notes

The authors declare no competing financial interest.

■ ACKNOWLEDGMENTS

P.L.P. gratefully acknowledges NSF funding (CHE-0804301) and helpful communications with Dr. Phil Klunzinger of Wavefunctions Inc., in the use of the SPARTAN program. I.I. and D.S.N. acknowledge DST, Government of India, for the financial support (project No.SR/S1/OC-54/2007). E.A.D. acknowledges the support of the Vanderbilt NSF-REU program (CHE 0850976). This work was conducted in part using the resources of the Advanced Computing Center for Research and Education at Vanderbilt University, Nashville, TN.

■ REFERENCES

(1) Haleema, S.; Sasi, P. V.; Ibnusaud, I.; Polavarapu, P. L.; Kagan, H. B. *RSC Adv.*, DOI: 10.1039/C2RA21205F.

(2) Nakahashi, A.; Miura, N.; Monde, K.; Tsukamoto, S. *Bioorg. Med. Chem. Lett.* **2009**, *19*, 3027−3030.

(3) Polavarapu, P. L. Determination of the Structures of Chiral Natural Products Using Vibrational Circular Dichroism. In *Comprehensive Chiroptical Spectroscopy*; Berova, N.; Polavarapu, P. L., Nakanishi, K.; Woody, R. W., Eds.; John Wiley & Sons: New York, 2012; Vol. 2, pp 387−420.

(4) Li, X.; Ferreira, D.; Ding, Y. *Curr. Org. Chem.* **2010**, *14*, 1678−1697.

(5) Nafie, L. A. *Nat. Prod. Comm.* **2008**, *3*, 451−466.
(6) Stephens, P. J.; McCann, D. M.; Devlin, F. J.; Smith, A. B., III *J. Nat. Prod.* **2006**, *69*, 1055−1064.
(7) Zuber, G.; Goldsmith, M. R.; Hopkins, T. D.; Beratan, D. N.; Wipf, P. *Org. Lett.* **2005**, *7*, 5269−5272.
(8) Giorgio, E.; Viglione, R. G.; Rosini, C. *Tetrahedron: Asymmetry* **2004**, *15*, 1979−1986.
(9) Autschbach, J. *Chirality* **2009**, *21*, E116−E152.
(10) Crawford, T. D.; Tam, M. C. *J. Phys. Chem. A* **2007**, *111*, 12057−12068.
(11) Goerigk, L.; Grimme, S. *J. Phys. Chem. A.* **2009**, *113*, 767−776.
(12) Devlin, F. J.; Stephens, P. J.; Cheeseman, J. R.; Frisch, M. J. *J. Am. Chem. Soc.* **1996**, *118*, 6327−6328.
(13) Helgaker, T.; Coriani, S.; Jorgensen, P.; Kristensen, K.; Olsen, J.; Ruud, K. *Chem. Rev.* **2012**, *112*, 543−631.
(14) Cossi, M.; Scalmani, G.; Rega, N.; Barone, V. *J. Chem. Phys.* **2002**, *117*, 43−54.
(15) Tomasi, J.; Mennucci, B.; Cammi, R. *Chem. Rev.* **2005**, *105*, 2999−3094.
(16) Mennucci, B.; Cappelli, C.; Cammi, R.; Tomasi, J. *Chirality* **2011**, *23*, 717−729.
(17) Scalmani, G.; Frisch, M. J. *J. Chem. Phys.* **2010**, *132*, 114110−114124.
(18) He, J.; Polavarapu, P. L. *J. Chem. Theory Comput.* **2005**, *1*, 506−514.
(19) Urbanova, M.; Setnicka, V.; Devlin, F.; Stephens, P. J. *J. Am. Chem. Soc.* **2005**, *127*, 6700−6711.
(20) Zhang, P.; Polavarapu, P. L. *J. Phys. Chem. A* **2007**, *111*, 858−871.
(21) Losada, M.; Tran, H.; Xu, Y. *J. Chem. Phys.* **2008**, *128*, 014508−1−014508−11.
(22) Nicu, P.; Heshmat, M.; Baerends, E. J. *Phys. Chem. Chem. Phys.* **2011**, *13*, 8811−8825.
(23) Devlin, F. J.; Stephens, P. J.; Osterle, C.; Wiberg, K. B.; Cheeseman, J. R.; Frisch, M. J. *J. Org. Chem.* **2002**, *67*, 8090−8096.
(24) He, J.; Polavarapu, P. L. *Spectrochimica Acta Part A: Mol. & Biomol. Spectroscopy* **2005**, *61*, 1327−1334.
(25) Polavarapu, P. L.; Scalmani, G.; Hawkins, E. K.; Rizzo, C.; Jeirath, N.; Ibnusaud, I.; Habel, D.; Nair, D. S.; Haleema, S. *J. Nat. Prod.* **2011**, *74*, 321−328.
(26) Polavarapu, P. L.; Donahue, E. A.; Shanmugam, G.; Scalmani, G.; Hawkins, E. K.; Rizzo, C.; Ibnusaud, I.; Thomas, G.; Habel, D.; Sebastian, D. *J. Phys. Chem A* **2011**, *115*, 5665−5673.
(27) Polavarapu, P. L.; Vijay, R. *J. Phys. Chem A* **2012**, *116*, 5112−5118.
(28) Boll, P. M.; Sorensen, E.; Balieu, E. *Acta Chem. Scand.* **1969**, *23*, 286−293.
(29) Glusker, J. P.; Minkin, J. A.; Soule, F. B. *Acta Crystallogr.* **1972**, *B28*, 2499−2505.
(30) Devlin, F. J.; Stephens, P. J.; Besse, P. *J. Org. Chem.* **2005**, *70*, 2980−2993.
(31) Frisch, M. J.; Trucks, G. W.; Schlegel, H. B.; Scuseria, G. E.; Robb, M. A.; Cheeseman, J. R.; Scalmani, G.; Barone, V.; Mennucci, B.; Petersson, G. A.; Nakatsuji, H.; Caricato, M.; Li, X.; Hratchian, H. P.; Izmaylov, A. F.; Bloino, J.; Zheng, G.; Sonnenberg, J. L.; Hada, M.; Ehara, M.; Toyota, K.; Fukuda, R.; Hasegawa, J.; Ishida, M.; Nakajima, T.; Honda, Y.; Kitao, O.; Nakai, H.; Vreven, T; Montgomery, J. A., Jr.; Peralta, J. E.; Ogliaro, F.; Bearpark, M.; Heyd, J. J.; Brothers, E.; Kudin, K. N.; Staroverov, V. N.; Kobayashi, R.; Normand, J.; Raghavachari, K.; Rendell, A.; Burant, J. C.; Iyengar, S. S.; Tomasi, J.; Cossi, M.; Rega, N.; Millam, J. M.; Klene, M.; Knox, J. E.; Cross, J. B.; Bakken, V.; Adamo, C.; Jaramillo, J.; Gomperts, R.; Stratmann, R. E.; Yazyev, O.; Austin, A. J.; Cammi, R.; Pomelli, C.; Ochterski, J. W.; Martin, R. L.; Morokuma, K.; Zakrzewski, V. G.; Voth, G. A.; Salvador, P.; Dannenberg, J. J.; Dapprich, S.; Daniels, A. D.; Farkas, Ö.; Foresman, J. B.; Ortiz, J. V.; Cioslowski, J.; Fox, D. J. *Gaussian 09*; Gaussian, Inc.: Wallingford, CT, 2009.
(32) Becke, A. D. *J. Chem. Phys.* **1993**, *98*, 5648−5652.
(33) Ditchfield, R.; Hehre, W. J.; Pople, J. A. *J. Chem. Phys.* **1971**, *54*, 724−728.
(34) Kendall, R. A.; Dunning, T. H., Jr.; Harrison, R. J. *J. Chem. Phys.* **1992**, *96*, 6796−6806.
(35) *SPARTAN '08*; Wavefunction, Inc.: Irvine, CA; www.wavefun.com/products/spartan.html.
(36) Options used with the SPARTAN program are CONF_SELECTION_RULE=5, WINDOW=20.0, SEARCHMETHOD=-THOROUGH, MMFF94 force field.
(37) Dr. Phil Klunzinger of Wavefunctions Inc. advised that a trick that is sometimes useful with the SPARTAN program to find twisted boat conformations is to select all 'waggable' carbon atoms and choosing a parameter of 3 (in the torsion window) for them. This procedure did find conformations with both positive and negative puckering angles for HADE but not for some other five-membered ring systems. Several literature papers that dealt with five-membered ring systems using SPARTAN did not seem to have made use of this option.
(38) *CONFLEX*; CONFLEX Corporation, AIOS Meguro 6F, 2-15-19, Kami-Osaki, Shinagawa-ku, Tokyo 141-0021, Japan; www.conflex.us.
(39) The options used with CONFLEX are the MMFF94S force field, SEL=20.0, SEARCH=ENERGY.
(40) Hori, K.; Dou, N.; Okano, K.; Ohgami, A.; Tsukube, H. *J. Comput. Chem.* **2002**, *23*, 1226−1235.
(41) Yanai, T.; Tew, D. P.; Handy, N. C. *Chem. Phys. Lett.* **2004**, *393*, 51−57.
(42) BHandHLYP Functional Implemented in the Gaussian 09 program.
(43) Polavarapu, P. L.; Shanmugam, G. *Chirality* **2011**, *23*, 801−807.
(44) Caricato, M.; Trucks, G. W.; Frisch, M. J.; Wiberg, K. B. *J. Chem. Theor. Comput.* **2010**, *6*, 370−383.